Changes in biofilm composition and microbial water quality in drinking water distribution systems by temperature increase induced through thermal energy recovery

Jawairia Imtiaz Ahmad [a,c,*], Marco Dignum [b], Gang Liu [a,d], Gertjan Medema [a,e,f], Jan Peter van der Hoek [a,b]

[a] Sanitary Engineering, Department of Water Management, Faculty of Civil Engineering and Geosciences, Delft University of Technology, P.O. Box 5048, 2600GA, Delft, the Netherlands
[b] Waternet, Korte Ouderkerkerdijk 7, 1096 AC, Amsterdam, the Netherlands
[c] Institute of Environmental Sciences and Engineering, School of Civil and Environmental Engineering, National University of Science and Technology, H-12 Sector, Islamabad, Pakistan
[d] Key Laboratory of Drinking Water Science and Technology, Research Centre for Eco-Environmental Sciences, Chinese Academy of Sciences, Beijing, 100085, PR China
[e] KWR Water Research Institute, P.O. Box 1072, 3430 BB, Nieuwegein, the Netherlands
[f] Michigan State University, 1405 S Harrison Rd, East-Lansing, 48823, USA

ARTICLE INFO

ABSTRACT

Drinking water distribution systems (DWDSs) have been thoroughly studied, but the concept of thermal energy recovery from DWDSs is very new and has been conceptualized in the past few years. Cold recovery results in a temperature increase of the drinking water. Its effects on drinking water quality and biofilm development are unclear. Hence, we studied both bulk water and biofilm phases for 232 days in two parallel pilot scale distribution systems with two temperature settings after cold recovery, 25 °C and 30 °C, and compared these with a reference pilot system without cold recovery. In all three pilot distributions systems (DSs) our results showed an initial increase in biomass (ATP) in the biofilm phase, along with occurrence of primary colonizers (*Betaproteobacteriales*) and subsequently a decrease in biomass and an increasing relative abundance of other microbial groups (amoeba resisting groups; *Xanthobacteraceae*, *Legionellales*), including those responsible for EPS formation in biofilms (*Sphingomonadaceae*). The timeline for biofilm microbial development was different for the three pilot DSs: the higher the temperature, the faster the development took place. With respect to the water phase within the three pilot DSs, major microbial contributions came from the feed water (17–100%) and unkown sources (2–80%). Random contributions of biofilm (0–70%) were seen between day 7–77. During this time period six-fold higher ATP concentration (7–11 ng/l) and two-fold higher numbers of high nucleic acid cells (5.20–5.80 × 10^4 cells/ml) were also observed in the effluent water from all three pilot DSs, compared to the feed water. At the end of the experimental period the microbial composition of effluent water from three pilot DSs revealed no differences, except the presence of a biofilm related microbial group (*Sphingomonadaceae*), within all three DSs compared to the feed water. In the biofilm phase higher temperatures initiated the growth of primary colonizing bacteria but this did not lead to differences in microbial diversity and composition at the end of the experimental period. Hence, we propose that the microbiological water quality of DWDSs with cold recovery should be monitored more frequently during the first 2–3 months of operation.

1. Introduction

Thermal energy recovery from drinking water distribution systems (DWDSs) is a novel and innovative concept. In the Netherlands the temperature within DWDSs stays between 4 and 10 °C in winter and between 15 and 20 °C in summer (Ahmad et al., 2020; Van der Hoek et al., 2018). This means that drinking water contains thermal energy, in the form of cold or heat, which provides opportunities to recover this

---

energy for cooling or heating purposes. In case of cold recovery, drinking water from the DWDS exchanges its cold inside a heat exchanger with a warm carrier medium (e.g. air, water, glycol, etc.) and slightly heated water flows back into the DWDS. According to a previous study, the theoretical potential of cold recovery from drinking water for the city of Amsterdam is around 2800 TJ/year while the energy required for space cooling for non-residential buildings in Amsterdam is estimated to be around 2161 TJ/year (Mol et al., 2011; Van der Hoek et al., 2018). So, in principle DWDSs harbour enough cooling capacity that could be recovered in the winter and stored underground, through an aquifer thermal energy storage, to provide space cooling in summers, or utilized directly in winters for facilities with extensive cooling requirements (e.g. blood banks, data centers, hospitals).

However, the cold transfer to the user, with subsequent heat transfer to the DWDSs, will cause the drinking water temperature to increase. Effects on chlorinated DWDSs have been studied recently (Zhou et al., 2020), but how this temperature increase will affect the microbiology in unchlorinated DWDSs has not been explored yet. These distribution systems have their distinctive micro-environments, where the biological stability of drinking water is maintained by limiting nutrient concentrations (El-Chakhtoura et al., 2015; Prest et al., 2016a; Van der Kooij, 1992; Van der Kooij and Van der Wielen, 2013). The microbial environment of DWDSs consists of loose deposits (Liu et al., 2014), suspended solids (Liu et al., 2013), water phase (Prest et al., 2016a, 2016b) and biofilm phase (Fish et al., 2016). Among these, biofilm and water phase contain the dominant part of the biomass (more than 80%) (Liu et al., 2017) in unchlorinated DWDSs. They contribute significantly in shaping the microbiome of drinking water during distribution (Hull et al., 2019; Ling et al., 2018). An increase in temperature after applying cold recovery might affect these habitats (water and biofilm), as temperature is a crucial environmental factor for microbial growth and community dynamics (Kelly et al., 2014; Rogers et al., 1994). Especially, growth of biofilms (Diaz Villanueva et al., 2011), proliferation of opportunistic pathogens (OPs) (Van Der Wende et al., 1989; Wingender and Flemming, 2011) like *Pseudomonas* and *Legionella* (Van der Kooij and Van der Wielen, 2013), occurrence of discolored water (Zhou et al., 2017) and sudden changes in microbial water quality parameters (like ATP and cell concentration) (Potgieter et al., 2018; Prest et al., 2016a) are linked with temperature changes. For this reason, it is highly important to investigate the effects of cold recovery on microbial water quality and biofilm characteristics to understand the impacts of full scale application in more detail. Currently the full scale application of cold recovery from drinking water (Sanquin in Amsterdam, the Netherlands) is set at a temperature of 15 °C after cold recovery to avoid any negative effects on the microbial quality of the water within DWDSs, but as a consequence it is not running at its full capacity in terms of energy recovery.

Hence, the current study was initiated with the goal to determine the potential changes in microbiology, both in terms of drinking water quality and microbiome, in DWDSs due to cold recovery. The study was carried out using pilot scale distribution systems. We studied two temperatures after cold recovery, 25 °C and 30 °C. The reason for choosing these two temperatures lies in the fact that the former is the maximum limit for the drinking water temperature within DWDSs in the Netherlands (Smeets et al., 2009; Staatscourant, 2011). In case no changes are observed at 25 °C, a temperature of 30 °C will significantly enhance the potential for cold recovery. However, this higher temperature may result in changes in microbiology. So, despite the fact that by Dutch law it is not allowed, the higher temperature was chosen as an extreme case for research purpose.

We hypothesized that the microbiology of DWDSs will be different after an increase in temperature of the water due to cold recovery application. For this purpose we studied both water and biofilm phases within pilot scale, unchlorinated drinking water distribution systems. Time series data of ATP concentrations, total cell concentrations, heterotrophic plate counts, *Aeromonas* spp., *Legionella* spp. and next

generation gene sequencing (NGS) were generated (over a period of 232 days) to determine changes in microbial community composition of both water and biofilm. Microbial source tracker was used in combination with the NGS data to determine the relative contribution of feed water and biofilm microbiology on drinking water microbiology coming out of the pilot scale distribution systems. This analysis of the interactions of biofilm and water phase at higher temperatures (after applying cold recovery) will help water companies to take into account the potential consequences of applying cold recovery on shaping the microbial water quality within DWDSs.

2. Materials and methods

2.1. Location and design of pilot scale distribution systems

Three pilot scale distribution systems (DSs) were designed and operated for almost 232 days from April till November 2018 (Fig. 1). The pilot scale DSs were situated at the drinking water treatment facility "Leiduin" of water utility Waternet near Amsterdam, and fed continuously with unchlorinated drinking water (Feed water (FW)) from this plant. Details of the treatment of the source water can be found in (Baghoth et al., 2011).

Among the three pilot scale DSs, DS-1 and DS-2 are the systems in which the temperature of the feed water was increased by using a heat exchanger (HE) to an elevated drinking water temperature of 30 °C and 25 °C respectively (HE description in supplementary information). After having passed the HE and having absorbed the heat to gain the maximum (T_{max}) set point temperatures of 30 and 25 °C, the heated drinking water flowed through the pipes and passed the whole length of the DSs. The set points were maintained throughout the entire experimental period, irrespective of changes in the feed water temperature due to seasonal variations. DS-3 is the reference system, where no heat exchanger was used and the temperature of the drinking water followed the seasonal variation of the source and treatment plant. This represents the Dutch non-chlorinated drinking water distribution systems. Throughout this study, it was used as a reference to DS-1 and DS-2.

Each pilot scale DSs had an internal diameter of 25 mm and a length of 30 m, and was made of polyvinyl chloride-unplasticised (PVC–U) pipes. For this experiment the flow rate was maintained at 4.5 l/min (flow velocity 0.15 m/s), which is based on typical flow velocities within Dutch drinking water distribution systems. All the DSs were equipped with flow and temperature sensors, for continuously monitoring the flow and temperature of the water. Dasy Lab software (version 13.0.1) was used for system monitoring and data logging. The difference between the temperature of the feed water and the temperature after cold recovery was termed as ΔT.

2.2. Sampling points and sampling frequency

For water sampling, small taps of PVC-U were installed within each pilot scale DSs (Fig. 1). During the study period, the water samples were taken every two weeks from each of the DSs at four sampling points: W_{fw} (feed water: treated/finished drinking water coming from the treatment plant), W_{25C}, $W30°C$ (after passing the heat exchangers) and W_{ref} (from the reference system). In total 64 (16 weeks × 4 points) water samples were taken and analysed. For biofilm sampling from the pipe surface, 30 cm long PVC-U coupons were designed and inserted in all three pilot DSs. These pipe sections have valves on both ends for easy removal. Duplicate biofilm samples were collected at different days of the study, starting from day 7 till day 232 (D_7, D_{14}, D_{28}, D_{49}, D_{84}, D_{140}, D_{232}). In total 42 biofilm samples were collected from the three pilot scale DSs (from DS-1 referred in this study as $Bf_{30°C}$, from DS-2 referred as $Bf_{25°C}$ and from DS-3 referred as Bf_{ref}). From each system, biofilm sampling was started from the distal end of the system in order to avoid disturbances within the systems related to the sampling procedure. For both water and biofilm samples, all microbiological analysis were performed
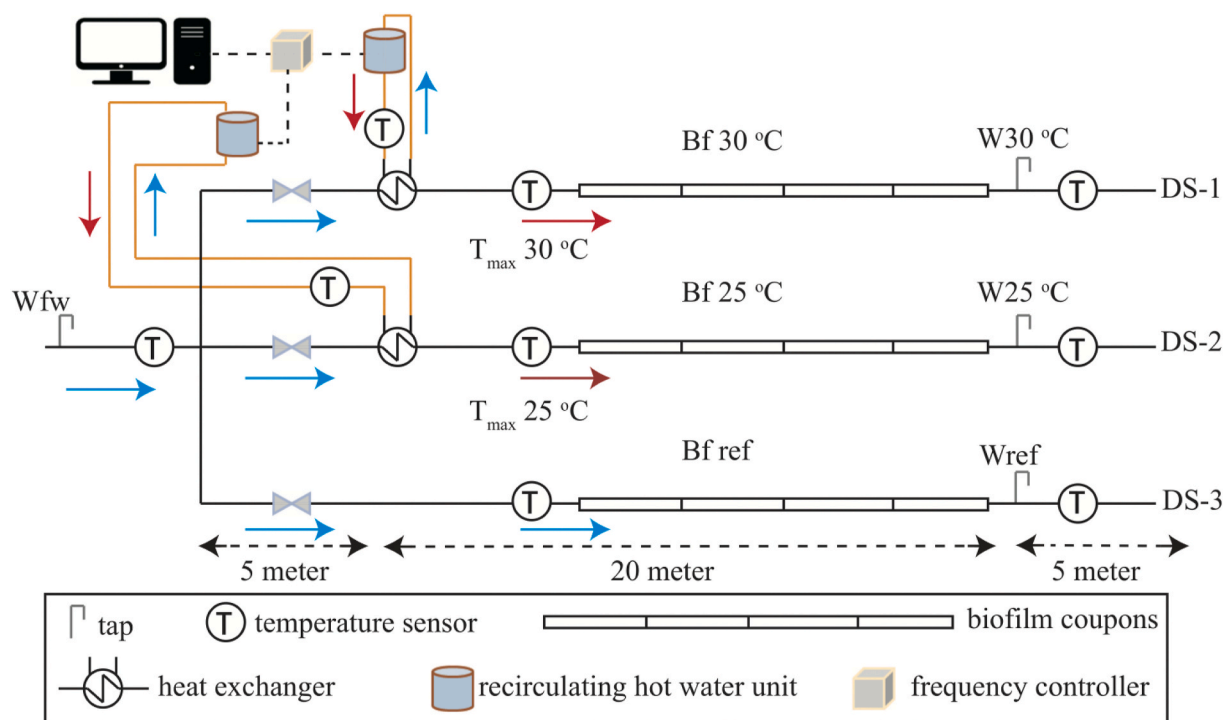
Fig. 1. Three, 30-m-long (each), pilot scale distribution systems (DSs) supplied with unchlorinated feed water, continuously for 24/7 for 232 days, to study the potential impacts of recovering cold. All the sampling sites for both water (W) and biofilm (Bf) samples were labelled. (W_{fw} = feed water, W_{ref} = water from reference system, $W_{25 C}$ = water after cold recovery (T_{max} = 25 °C), $W_{30°C}$ = water after cold recovery (T_{max} = 30 °C), Bf_{ref} = biofilm from reference system, $Bf_{25°C}$ = biofilm formed after cold recovery (T_{max} = 25 °C), $Bf_{30°C}$ = biofilm formed after cold recovery (T_{max} = 30 °C).

within 24 h of sampling.

2.3. Biofilm samples preparation

For biofilm analysis, the valves on both sides of the pipe coupons were closed and the coupons were taken out of the systems and filled with 30 ml of DNA-free water. To remove the biofilm from the coupons, the pipe coupons were pretreated by ultra-sonication, at a frequency of 40 KHz, in a water bath (Ultrasonic 8800, Branson, USA) for 2 min. This sonication procedure was repeated twice (Liu et al., 2014; Magic-Knezev and van der Kooij, 2004). The obtained suspension of 90 ml was used for further analysis, and results for each measured parameter were normalized based on the surface area of the pipe coupon (236 cm^2) and the obtained suspension volume.

2.4. Analyses

2.4.1. Dissolved organic carbon (DOC), heterotrophic plate count (HPC), Aeromonas and Legionella spp.

From both water and biofilm samples cultivable bacteria (HPC), *Aeromonas* spp. and *Legionella* spp. were analysed according to the Dutch standard procedures for these parameters (NEN-6222, NEN-6263 and NEN-6265 respectively), as described in (Van der Kooij et al., 2018). Dissolved organic carbon (DOC) was measured only from water samples according to the Dutch procedure (NEN-1484) (Zlatanović et al., 2017).

2.4.2. Adenosine triphosphate and total cell count

Bacterial cell numbers and active biomass were determined by measuring cell counts and the total adenosine triphosphate (ATP) concentration from both biofilm (n = 42) and water (n = 64) samples. Cell counts were measured by a flow cytometer (C6-Flowcytometer, Accuri Cytometers, USA) using the same protocol that was previously developed and tested for drinking water samples (Prest et al., 2013). Total and membrane-intact cell counts were distinguished by adding two stains

simultaneously as described by Prest et al. (2013). LNA and HNA cells were distinguished by applying the same electronic gating strategy as described by Prest et al. (2013). Active biomass was determined by measuring total ATP concentrations from both biofilm and water samples using a reagent kit for bacterial ATP and a luminometer (Celsis Advance Luminometer, Charles River, USA), as described previously (Magic-Knezev and van der Kooij, 2004).

2.4.3. DNA extraction and 16S rRNA gene sequencing

To examine the microbiome of the pilot scale DSs, DNA was extracted using a DNeasy PowerBiofilm kit (Qiagen, USA) from both water samples (n = 64) and biofilm samples (n = 42). Each sample (for water, a volume of 2 L and for biofilm, 30 ml suspension from each sample) was filtered through a 47 mm polycarbonate filter (0.22 μm pore size, Sartorius, Germany). Subsequently the filters were stored at −20 °C and further used for DNA extraction according to the mentioned protocol. For 16S rRNA gene sequencing, the V3–V4 region of the 16S rRNA gene was amplified using primers 341F: 5'-CCTACGGGNGGCWGCAG-3' and 785R: 5'-GACTACHVGGGTATC-TAATCC-3' (Thijs et al., 2017). Paired-end sequence reads were generated using the Illumina MiSeq platform. FASTQ sequence files were generated using the Illumina Casava pipeline version 1.8.3. The initial quality assessment was based on data passing the Illumina Chastity filtering. Subsequently, reads containing the PhiX control signal were removed using an in-house filtering protocol at BaseClear laboratory, Leiden, the Netherlands. In addition, reads containing (partial) adapters were clipped (up to a minimum read length of 50 bp). The second quality assessment was based on the remaining reads using the FASTQC quality control tool version 0.10.0, where low quality sequence ends were removed (Quality score = 30) and remaining sequences were used further downstream to analyse Bioinformatics. All sequencing files were deposited in the sequence read archive of the NCBI (National Center for Biotechnology Information) under the accession number PRJNA613992.

2.4.4. Sequence data processing and statistical analysis

The obtained sequence libraries after quality control from FASTQC were imported into the Quantitative Insights into Microbial Ecology (QIIME2) (version 2019.7) pipeline (Bolyen et al., 2019). The sequences were further screened (at the maximum length of 298 bp), denoised, paired ends were merged and chimeras were removed using the inbuilt, Divisive Amplicon Denoising Algorithm 2 (DADA2) (Callahan et al., 2016). The remaining representative sequences were clustered to operational taxonomic units (OTUs) at an identity of 97%. For taxonomic assignment, feature-classifier plugin in QIIME2 (2019.7) was used against the SILVA database (132 release) for determining the microbial community composition at different taxonomic levels. Further, core microbial community was defined based on OTUs which were present among at least 80% of the samples (in the water phase) and in both duplicates in the biofilm samples, with a relative abundance higher than 1%. The taxa bar plots were generated based on core OTUs at different taxonomic levels of Class, Family and Order.

Both alpha (Shannon, observed OTUs, pielou's eveness) and beta (Jaccard distance matrix and weighted Unifrac) diversity indices were calculated using phylogenetically based rooted tree (generated by aligning sequences using MAFFT plugin for phylogenetic reconstruction in FastTree) and with a sampling depth of 2000 sequences using QIIME2 diversity plugin. Principal coordinate analysis (PCoA) plots were generated using Jaccard and weighted distance matrix in emperor plot plugin.

Single factor ANOVA and pearson correlation were performed in Microsoft Excel for mac (version 15.40), to determine the significance of differences between quantitative microbial parameters (ATP, TCC, HPC, DOC) and correlation of these parameters with feed water temperature and ΔT, for both DS-1 and DS-2.

2.4.5. Source tracker for microbial source tracking of bulk water from DSs

After assigning the taxonomic classification, the obtained OTU table was used as input for microbial source tracking of effluent water from the three pilot DSs (W_{25oC}, W_{30oC}, W_{ref}). The source tracker method was previously described by (Knights et al., 2011). The method identifies the extent of contributions of each source to a designated sink by comparing their community fingerprinting. The obtained results show the percentage contribution of each source to the sink. In this study feed water and biofilms from each respective DS were defined as sources and effluent water from each pilot DS on a particular sampling day was defined as sink (Table S1). The analysis was performed using default
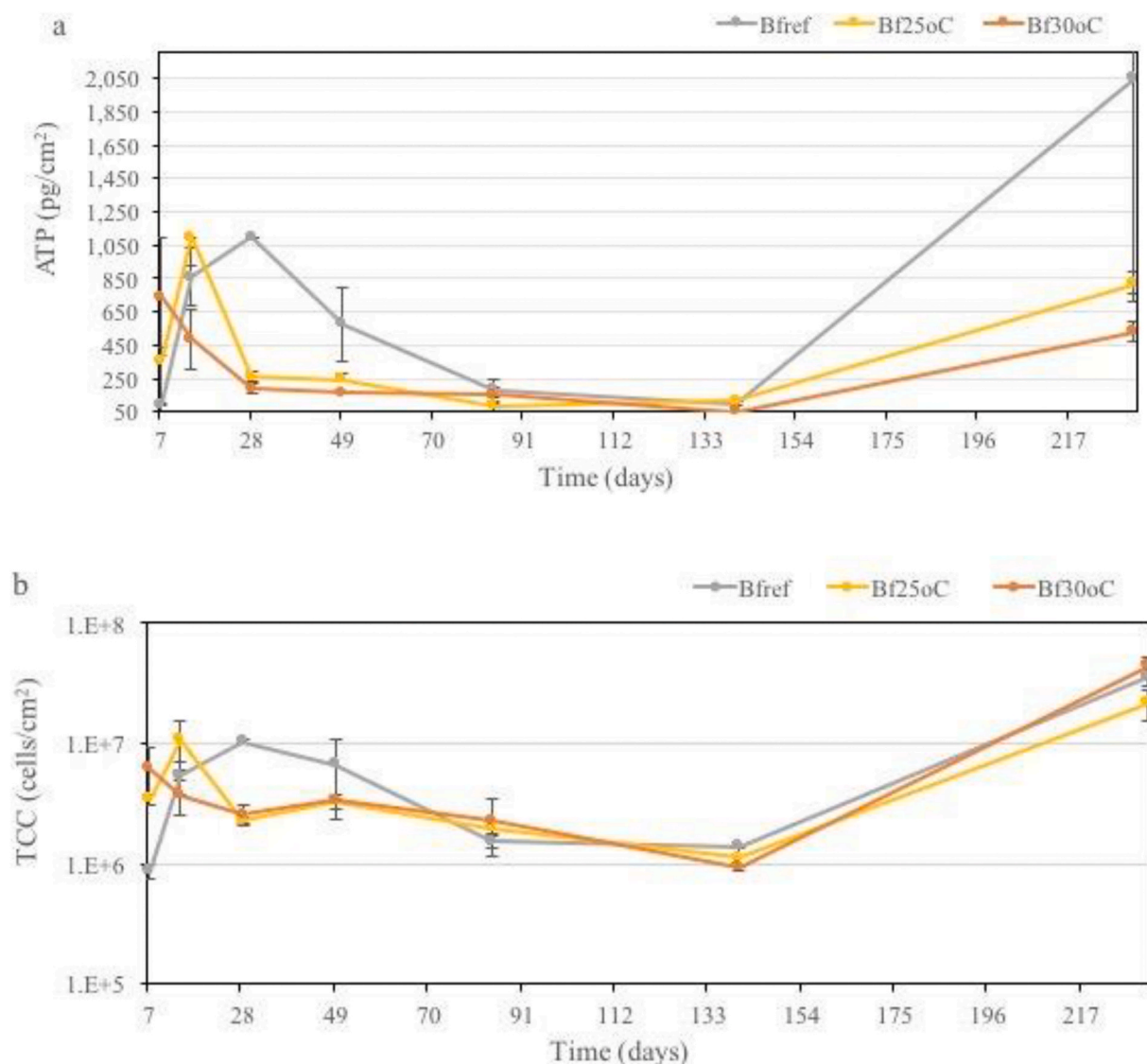

Fig. 2. Biomass formation measured in terms of ATP (a) and cell concentration (b), from biofilms formed over the period of 232 days, within three pilot distribution systems (Bf$_{ref}$ = biofilm from reference system, Bf$_{25°C}$ = biofilm formed after cold recovery (T_{max} = 25 °C), Bf$_{30°C}$ = biofilm formed after cold recovery (T_{max} = 30 °C)).

settings with a rarefaction depth of 1000, burn-in 100, restart 10, alpha (0.001), and beta (0.01) Dirichlet hyper parameter. The analysis was performed with QIIME software and percentages were calculated as previously described and also applied for drinking water communities by (Liu et al., 2018).

3. Results

3.1. Microbial activity in the biofilm phase

The three pilot distribution systems showed similar patterns of biofilm development both in terms of ATP and cell concentration (Fig. 2a and b). Growth reached an initial maximum biomass within the first 28 days, then decreased to a minimum on day 140 and finally increased till day 232, at the end of sampling.

On day 7, the ATP in Bf_{ref} was 95 ± 3 pg/cm^2, and continued to grow till day 28. It reached a maximum biomass concentration of 1100 pg/cm^2 and then decreased to a minimum on day 140 (100 pg/cm^2), and subsequently reached a maximum of 2050 ± 1000 pg/cm^2 on day 232.

The latter measurement showed a large difference between the duplicates. For $Bf_{25°C}$, the same maximum level in ATP was observed earlier on day 14, which then decreased to a minimum of 115 pg/cm^2 on day 140, and increased again to 815 ± 77 pg/cm^2 on day 232. The maximum ATP in $Bf_{30°C}$ was observed on day 7 (740 ± 300 pg/cm^2) and decreased from day 7 through day 140 (53 ± 7 pg/cm^2) and reached an increased final concentration on day 232 (530 ± 56 pg/cm^2).

Similar to the growth patterns of ATP, an initial maximum cell concentration was observed in the Bf_{ref} on day 28 (1×10^7 cells/cm^2), then a minimum was observed on day 140 (1×10^6 cells/cm^2) and an increased final cell concentration (3×10^7 cells/cm^2) was observed on day 232. In $Bf_{25°C}$ a maximum cell concentration was measured on day 14 (1×10^7 cells/cm^2), a minimum on day 140 (1×10^6 cells/cm^2) and a final concentration of 2×10^7 cells/cm^2 on the last day of sampling. $Bf_{30°C}$ showed an initial maximum cell concentration of 6×10^6 cells/cm^2 on day 7, which then decreased to a minimum on day 140 (9×10^5 cells/cm^2) and finally an increase was observed on day 232 (4×10^7 cells/cm^2) (Fig. 2b). Interestingly, from day 28 through day 232 the $Bf_{25°C}$ and $Bf_{30°C}$ showed comparable cell concentrations (Fig. 2b), intact
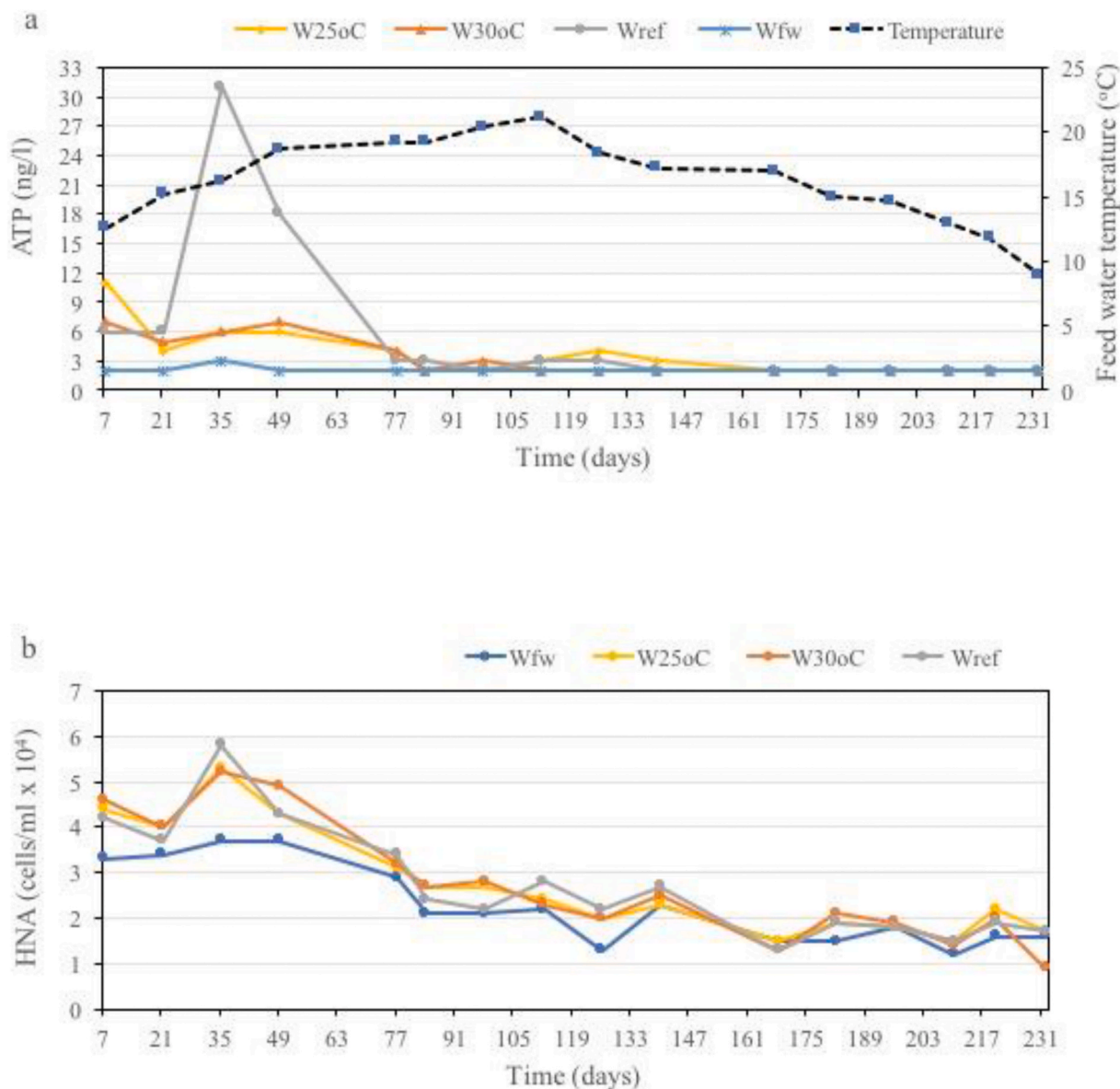

Fig. 3. Microbiological water quality measured by ATP (a) and high nucleic acid cells (b), from feed water (W_{fw} = feed water) and all three sampling sites from pilot distribution systems (W_{ref} = water from reference system, W_{25oC} = water after cold recovery (T_{max} = 25 °C), W_{30oC} = water after cold recovery (T_{max} = 30 °C)).

cell counts (1×10^6–6×10^6 cells/cm^2) and HPC counts (3×10^4–2×10^4 cells/cm^2) (data not shown here). Later on, from day 84 till day 232 a comparable microbial cell concentration was found within all three biofilms.

Legionella spp. and *Aeromonas* spp. were not found in the biofilms using plate counts, neither in the situation with cold recovery, nor in the situation without cold recovery. They were absent in the feed water and no growth was observed in the biofilms.

3.2. Microbial activity in bulk water phase

During the experimental period, the temperature of the W_{fw} ranged from 8.9 to 21.2 °C and ΔT for $W_{30°C}$ and $W_{25°C}$ was between 9 and 21 °C and 4 and 19 °C respectively (Table S2). Irrespective of the seasonal variations in water temperature, the feed drinking water used for this experiment was biologically stable with Assimilable Organic Carbon (AOC) concentrations below 10 ± 2 μg-C/l (data from Waternet). DOC ranged between 1.2 and 2.0 mg C/l (Fig. S1). The ATP (Fig. 3a) and total cell concentration (Fig. S2a) of W_{fw} varied between 2 and 3 ng/l and 1.00–1.80×10^5 cells/ml, respectively, the observed HPC were between 2 and 20 cfu/ml (Fig. S2c).

From day 7 to day 77, ATP levels in the effluent drinking water from all three DSs were higher than in the feed water (Fig. 3a). This was most pronounced in W_{ref}, where a maximum ATP concentration was observed on day 35 (31 ng/l), followed by a decrease till day 77 (3 ng/l). Later on, a more or less stable ATP concentration (2–3 ng/l) was observed between day 84 and the final sampling day 232. The maximum ATP concentration in the $W_{25°C}$ (11 ng/l) and $W_{30°C}$ (7 ng/l) was measured on day 7, a decrease on day 77 (4 ng/l) and a final ATP concentration of 2 ng/l on day 232.

Overall, from all four sampling sites of water, the total cell concentration (Fig. S2a) remained higher from day 7 to day 77 (1.70–1.90×10^5 cells/ml) and later on a stable and lower cell concentration was observed till day 232 (7.60×10^4–1.10×10^5 cells/ml). Similar to the results of ATP, high nucleic acid (HNA) cells increased considerably within $W_{30°C}$, $W_{25°C}$ and W_{ref} compared to W_{fw} between day 7 and 49 (Fig. 3b). From all three DSs maximum HNA cells (5.20–5.80×10^4 cells/ml) were observed on day 35, then decreased to 2.40–2.70×10^4 cells/ml on day 84 and reached a final concentration of 9×10^3–1.70×10^4 cells/ml on day 232. Regarding low nucleic acid (LNA) cells, no differences between sampling sites were observed but overall a decreasing trend in total LNA cells was noticed in all water samples (Fig. S2b), along with a decrease in W_{fw} temperature (Pearson's r = 0.5). The heterotrophic plate counts (Fig. S2c) showed an increase in the colony forming units within the three systems compared to the W_{fw} and significant (p < 0.05) differences in HPC were observed between all four water sampling sites (W_{fw}, $W_{30°C}$, $W_{25°C}$ and W_{ref}).

Legionella spp. and *Aeromonas* spp. were not detected from the W_{fw} and no regrowth was observed after applying cold recovery ($W_{25°C}$, $W_{30°C}$) or within W_{ref} (results not shown).

3.3. Microbial diversity and biofilm composition

The biofilm was characterized by a steady increase in species diversity (shannon diversity index) and evenness (pielous' e). With respect to observed taxonomic units (OTUs), very few numbers of OTUs were observed from biofilm samples on day 7 (Fig. S3a), with higher numbers observed in Bf_{ref} (34 ± 3) compared to $Bf_{25°C}$ (18 ± 4) and $Bf_{30°C}$ (20 ± 4). In the Bf_{ref} a decrease in OTUs was noticed from day 7 to day 14 (25 ± 7), and later an increase from day 28 to day 232, by reaching the maximum number of 266 ± 30 OTUs. In the $Bf_{25°C}$ and $Bf_{30°C}$ OTUs were increasing between day 7 and day 232 and reached a maximum of 289 ± 4 and 245 ± 30 OTUs, respectively. Overall $Bf_{30°C}$ showed lower numbers of OTUs compared to $Bf_{25°C}$ and Bf_{ref}. In terms of species diversity (Fig. S3b) and evenness (Fig. S3c), Bf_{ref} was steadily increasing from day 7 (diversity: 1.2 ± 0.7, evenness: 0.2 ± 0.1) and reached its

maximum on day 232 (diversity: 7.3 ± 0.2, evenness: 0.9 ± 0.01). $Bf_{25°C}$ and $Bf_{30°C}$ were more diverse (1.6–1.8) and even (0.4) at day 7 compared to Bf_{ref}, then steadily increased and reached a maximum on day 49 (diversity: 5.3–5.6, evenness: 0.7–0.8). Then a decrease was observed between day 49 and day 84, and an increased final diversity (7.2–7.4) and evenness (0.9) was measured on day 232.

In total, four core Phyla were observed (Table S3a) comprising 95–100% of the microbial communities among all biofilms, on different days. As shown in Fig. S4, *Proteobacteria* was the most dominant phylum constituting almost 90–100% of the microbial community between day 7 and day 28 in $Bf_{25°C}$ and $Bf_{30°C}$, and till day 49 in Bf_{ref}. The four dominantly observed classes were *Gammaproteobacteria* (30–95%), *Alphaproteobacteria* (1–50%), *Planctomycetacia* (1–6%) and *Deltaproteobacteria* (1–5%), simultaneously over the period of time. From day 7 till day 232, the relative abundance of *Gammaproteobacteria* was decreasing and three other classes (*Alphaproteobacteria, Planctomycetacia, Deltaproteobacteria*) were increasing in abundance respectively (Fig. S4).

At the Order level, *Betaproteobacteriales* (Fig. 4a), was most abundant in $Bf_{25°C}$ (88%) and $Bf_{30°C}$ (87%) on day 7 and in Bf_{ref} (82%) on day 14. During day 7–49, at Family level (Fig. 4b), the community composition data showed *Burkholderiaceae* (member of order *Betaproteobacteriales*) and *Sphingomonadaceae* as the most dominant microbial groups among all three biofilms (Bf_{ref}, $Bf_{25°C}$ and $Bf_{30°C}$). Where the highest relative abundance of *Burkholderiaceae* was observed on day 7 within all biofilms (Bf_{ref}: 78%, $Bf_{25°C}$: 87%, $Bf_{30°C}$: 86%), its relative abundance decreased over time. *Sphingomonadaceae* was observed in $Bf_{25°C}$ (6%) and $Bf_{30°C}$ (8%) starting from day 7 and in Bf_{ref} (13%) on day 14. The relative abundances of *Burkholderiaceae* and *Sphingomonadaceae* were gradually decreasing when biofilms became more diverse with the presence of other microbial groups, such as *Xanthobacteraceae,* which was observed in $Bf_{25°C}$ and $Bf_{30°C}$ on day 28 and in Bf_{ref} on day 49 with the relative abundances of 3% and 1%, respectively. Simultaneously, occurrence of *Legionellales* in $Bf_{30°C}$, $Bf_{25°C}$ and in Bf_{ref} (1%) on day 28, 49 and 84 respectively was noticed. Among other groups the higher relative abundance of *Pseudomonadaceae* was observed on day 7 in Bf_{ref} (17%) and $Bf_{25°C}$ (5%), and on day 140 in $Bf_{30°C}$ (15%). Overall, six core taxa (Table S3b) were observed in biofilm samples belonging to these dominant microbial groups.

3.4. Microbial diversity and composition of bulk water

Based on gene sequencing analysis of drinking water samples from the feed water and effluent water coming out of the three DSs ($W_{25°C}$, $W_{30°C}$ and W_{ref}), the OTUs, shannon diversity and community evenness were fluctuating considerably over the course of this study and largely followed a varying pattern of the feed water (Fig. S5a). From day 7 through day 182 more fluctuations were observed in numbers of OTUs, with an average number of OTUs ranging from 141 to 200 and with a very high standard deviation of 107–179. In contrast, comparatively stable numbers of OTUs were observed from day 196 through day 232, ranging between 58 ± 25 and 87 ± 82. Similar results were observed for the other alpha diversity metrices like shannon diversity index (Fig. S5b) and pileou's evenness (Fig. S5c). These metrices showed a more diverse (Shannon index: 5.1 ± 2.5) and noticeably even (pielou's e: 0.7 ± 0.2) microbial community from day 7 to day 182, and a relatively less diverse (Shannon index: 3.5 ± 1) and less even (pielou's e: 0.5 ± 0.1) but comparatively more stable/consistent community from day 196 to day 232.

Furthermore, the community composition data revealed similar patterns as the community diversity indices. In total, three core phyla were detected from W_{fw} and W_{ref}, five from $W_{25°C}$, and four from $W_{30°C}$ (Table S4a). Five major classes were observed (Fig. S6), comprising 20–100% of the total microbial communities in all water samples. The most dominant were *Gammaproteobacteria*, *Parcubacteria* and *Alphaproteobacteria* in W_{fw} and W_{ref}. In $W_{25°C}$ and $W_{30°C}$ two additional classes were also observed, namely *Subgroup 6* (Phylum *Acidobacteria*) and
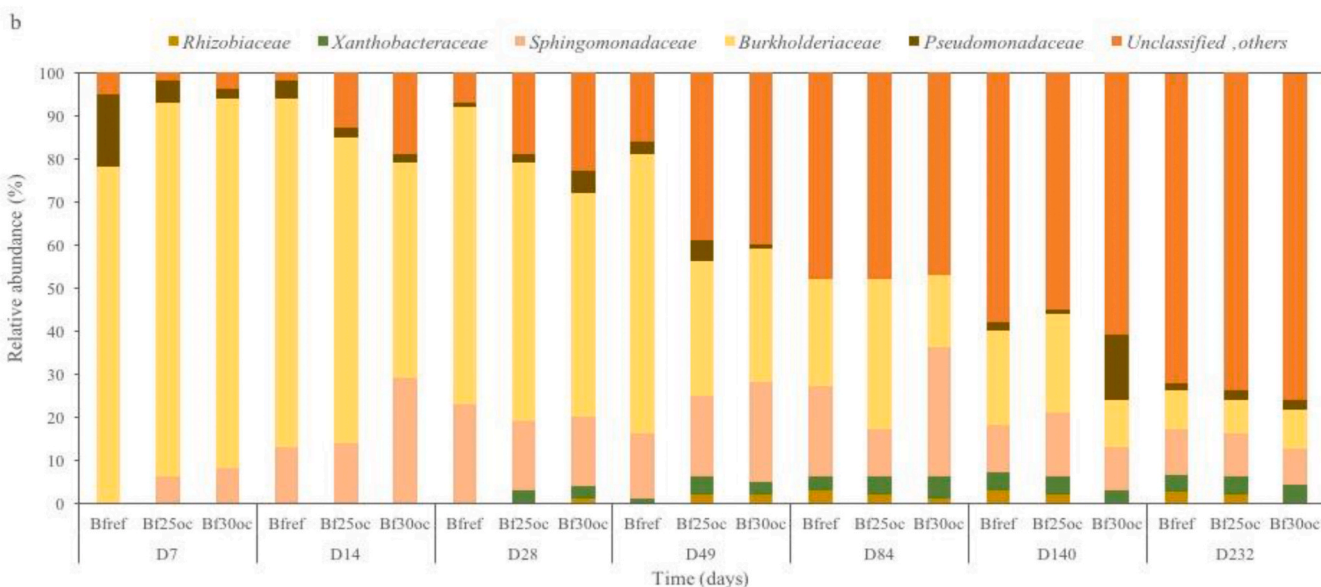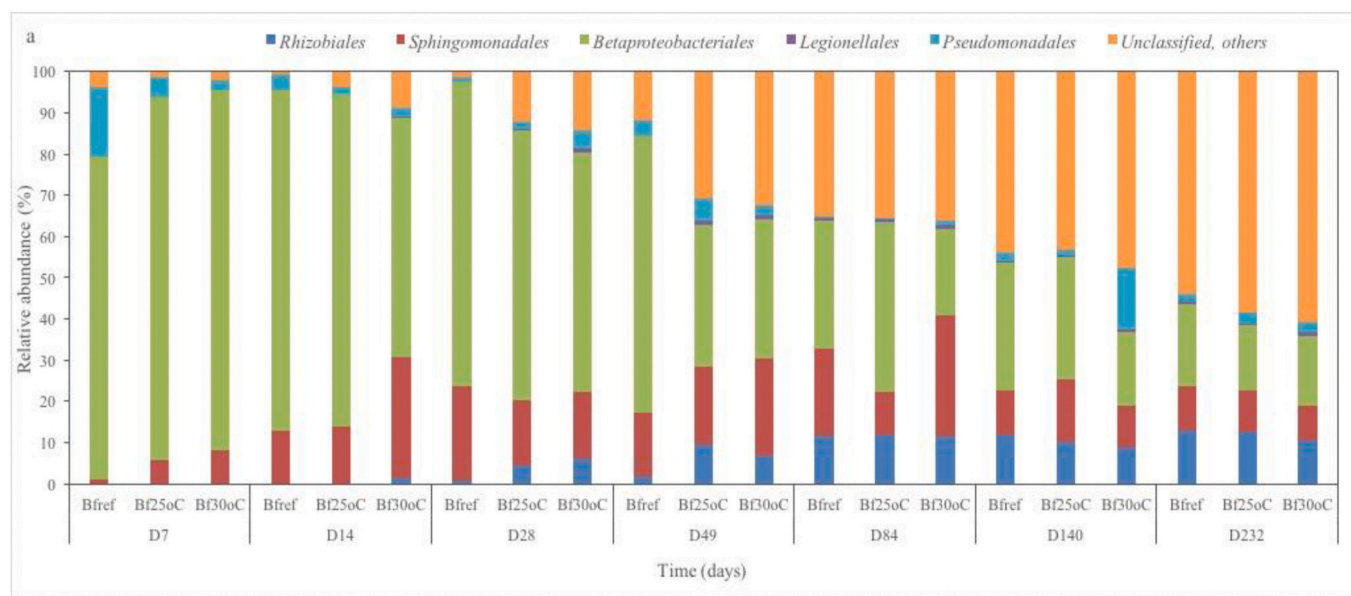
Fig. 4. Microbiome of biofilms shown as relative abundances (%) of core microbial groups, at both Order (a) and Family (b) level of taxonomic classification, from three sampling locations, developed within pilot distribution systems (Bf$_{ref}$ = biofilm from reference system, Bf$_{25°C}$ = biofilm formed after cold recovery (T$_{max}$ = 25 °C), Bf$_{30°C}$ = biofilm formed after cold recovery (T$_{max}$ = 30 °C)).

Actinobacteria.

At Family level of taxonomic classification, four major microbial groups were observed in all water samples (Fig. 5), with *Burkholder-iaceae* (10–80%) and *Pseudomonadaceae* (10–70%) as the most dominant groups, followed by *Methylophilaceae* (4–40%). *Sphingomonadaceae* was only observed in samples from W$_{25°C}$ (1–9%), W$_{30°C}$ (1–8%) and W$_{ref}$ (1–3%), starting from day 7 through day 232. *Pseudomonadaceae* (5–69%) was observed at all sampling points and its relative abundance was higher in W$_{25°C}$, W$_{30°C}$ and W$_{ref}$ compared to W$_{fw}$, between day 7 and day 77. Later on, no pattern was observed for its occurrence. Also, periodically a higher relative abundance of *Burkholderiaceae* was measured in W$_{fw}$ between day 7 and 182, but W$_{25°C}$, W$_{30°C}$ and W$_{ref}$

showed comparatively less variation in its abundance during this time period.

Overall, very few (<10) core taxa (relative abundance >1% and present in 80% of the samples from each sampling location) were observed from water samples. All of those were belonging to the above mentioned microbial groups, from all water sampling locations (Table S4b). Comparatively, more taxa were detected from the water phase after applying cold recovery (W$_{25°C}$, W$_{30°C}$) than from the reference and feed water (W$_{ref}$ and W$_{fw}$).
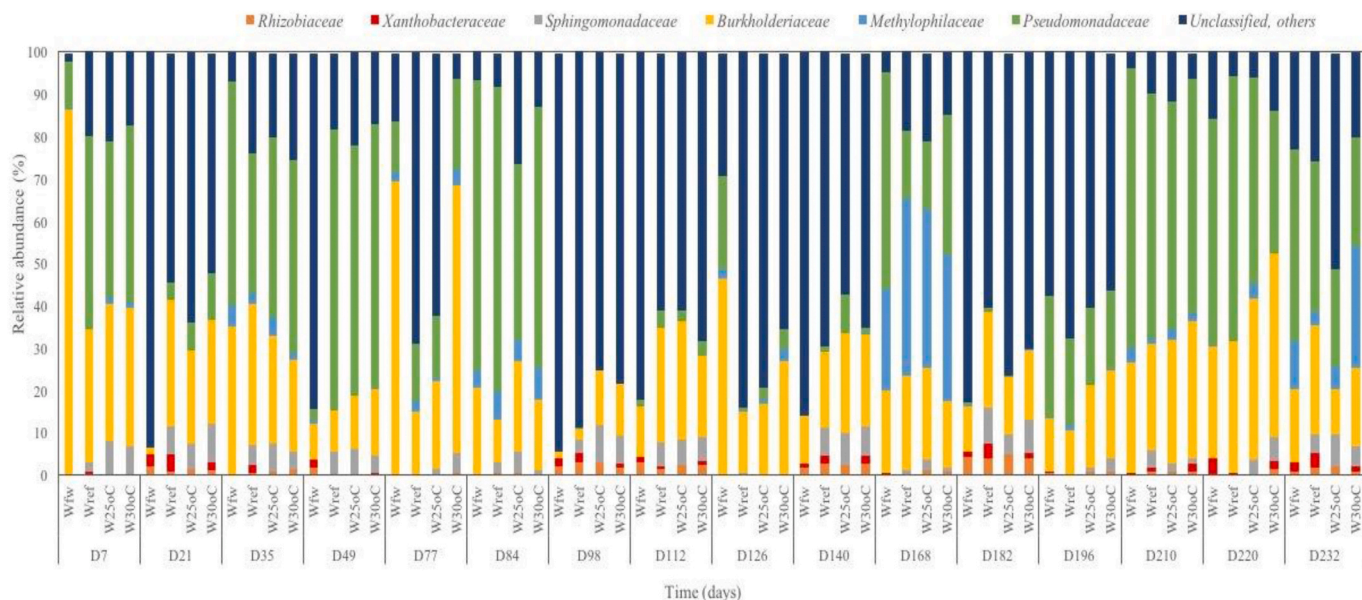
Fig. 5. Microbiome of drinking water, represented by relative abundances (%) of core microbial groups, at family level of taxonomic classification. From all four studied sampling sites (W_{fw} = feed water, W_{ref} = water from reference system, $W_{25}o_C$ = water after cold recovery (T_{max} = 25 °C), $W_{30}o_C$ = water after cold recovery (T_{max} = 30 °C)).

3.5. Source tracking of bulk water communities within three DSs

For the microbial communities of bulk water coming out of the three DSs (W_{ref}, $W_{25}o_C$, $W_{30}o_C$), feed water (W_{fw}) and biofilm (Bf_{ref}, $Bf_{25°C}$, $Bf_{30°C}$) bacterial communities were treated as potential sources. Within all three DSs, W_{fw} was the main contributor towards the microbial bulk water communities, along with contributions from unknown sources. Within all three pilot DSs, the contributions of biofilm communities to the bulk water microbial community showed a random pattern but it was corresponding with the initial higher ATP and HNA cell concentrations of bulk water. At the start, the biofilms made an initial maximum contribution, then the contribution decreased and finally

increased, except for the 30 °C system where the decrease and increase were observed twice (Fig. 6).

The results obtained from the source tracker for the W_{ref} showed the W_{fw} as the main contributor (52–100%) from day 7 till day 232 and the contributions of W_{fw} were varying over time based on the contribution from unkown sources (3–38%) and from Bf_{ref}. The latter has an input of 20% on day 7 and a maximum contribution on day 49 (68%). The contribution of Bf_{ref} decreased between day 77 and day 84 (0–4%) and was increasing again from day 98 (12%) to day 182 with a contribution of 26%. Later on, from day 196 till day 232 W_{fw} was observed to contribute 62–100%.

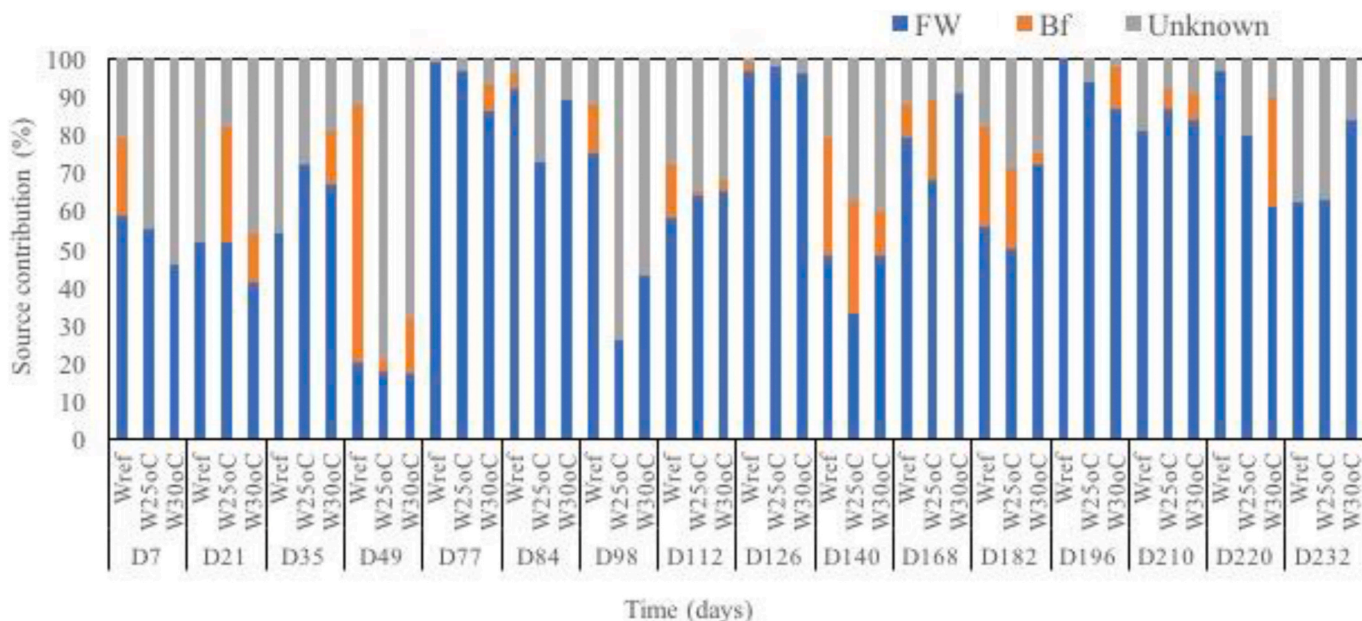In the $W_{25}o_C$, feed water also made the major contributions

Fig. 6. The results of source tracker method, showing percent contributions of microbial communities from different sources (feed water = FW, biofilm from relevant pilot DS = Bf, Unkown sources) into sinks (W_{ref} = water from reference system, $W_{25}o_C$ = water after cold recovery (T_{max} = 25 °C), $W_{30}o_C$ = water after cold recovery (T_{max} = 30 °C)) on each water sampling day.

(26–98%) and the contributions from unknown sources ranged from 2 to 79% over the study period. $Bf_{25°C}$ made the highest contribution on day 21 (30%) and a decrease or no contribution was observed from day 35 till day 126. Then an increase was seen from day 140–182 (21–30%) and a final contribution of 5% on day 210.

In the $W_{30°C}$ from day 7 to day 232, feed water contributions ranged from 17 to 96% and the unknown sources were contributing 2–57%. The $Bf_{30°C}$ had a maximum contribution from day 21 to day 77 (7–15%), then a decrease or no contributions from day 84 to day 126 and again an increase was observed on day 140 (12%). Later on, a decrease or no contribution was seen on day 168, then an increase was observed on day 182, and a final contribution of 29% on day 220.

4. Discussion

4.1. Influence of cold recovery on the early growth and development of biofilms

The microbiological characteristics of the DWDSs have been studied widely and thoroughly both for chlorinated (Douterelo et al., 2013; Potgieter et al., 2018) and unchlorinated systems (Prest et al., 2016b; Vital et al., 2012). The current study focused on the microbial impacts of application of a new technology, cold recovery, within unchlorinated systems. Especially development and growth of the biofilms were studied dynamically over time to trace changes during their formation, as biofilms are the micro-environments which are thought to be long-term residents (from days to decades) within DWDSs (Flemming et al., 2016; Henne et al., 2012; Van Der Wende et al., 1989). Bacterial biofilm development on pipe surfaces are characterized by a series of developmental stages, which includes: 1) initial preconditioning of surface (recruitment of organic substances from bulk water; as soon as (minutes/hours) the surface is exposed to flowing water, on which bacteria will attach), 2) attachment of primary colonizers, 3) growth of attached bacteria, 4) protozoans grazing and 5) finally detachment of bacterial cells from biofilm into the flowing bulk water (Mathieu et al., 2019).

Development of biofilms at different temperatures has not yet been studied inside DWDSs, but a study on river water has reported an acceleration of microbial colonization at higher temperatures (Diaz Villanueva et al., 2011). Similarly, we observed here temperature as a controlling factor for the initial growth of biofilms within unchlorinated pilot DSs, not only by accelerating the primary colonization (higher relative abundance of *Betaproteobacteriales* starting from day 7) of microbes within biofilms, grown at 30 °C (Fig. 4), but also by enhancing the early biomass formation in the biofilms, developed at 30 °C after cold recovery, which grew faster at the beginning (day 7), in terms of ATP and TCC (Fig. 2). At the higher temperature, the peaks in biofilm development (ATP and TCC) during the first 50 days occurred earlier. The biofilm at 30 °C became more diverse and complex in microbial community composition earlier (day 14) compared to the biofilms which were grown at lower ($Bf_{25°C}$ on day 28) and fluctuating (Bf_{ref} on day 49) temperatures (Fig. 4).

The biofilms that developed in all three pilot DSs, although following an independent timeline for their development, showed an increase in biomass, along with occurrence of primary colonizers (*Betaproteobacteriales*) and consequently a decrease in biomass and an increasing relative abundance of other microbial groups (amoeba resisting groups; *Xanthobacteraceae*, *Legionellales*), including those responsible for EPS formation in biofilms (*Sphingomonadaceae*) which protects them from outer stresses (Balkwill et al., 2006; Fish et al., 2016). This biomass decrease was possibly related to protozoan grazing within the first 50 days (Van der Kooij et al., 2018), which was observed on day 28 in $Bf_{25°C}$ and $Bf_{30°C}$, and on day 49 in Bf_{ref} (Fig. 2 a and b). Later in time, biofilms reached a more even/mature state of growth (Henne et al., 2012), in terms of microbial diversity and abundance, which has been observed here around day 49 for biofilms grown after cold recovery (25 °C, 30 °C)

and day 84 for reference biofilms (Fig. S3).

The microbial similarities among biofilms after day 84 showed that feed water quality and composition determines the microbial diversity and composition of more stable/mature biofilms (Ling et al., 2015; Neu et al., 2019). The environmental conditions (Rogers et al., 1994) (temperature in this case) only play a significant role during early primary colonization and growth of microbes, where differences in microbial composition and biomass were observed among the three pilot DSs.

4.2. Influence of biofilm development on pipe surface on bulk water characteristics

In the first few months of operation (7–77 days), the amount of biomass, as measured by ATP and specifically the number of high nucleic acid (HNA) cells in the bulk water from all three DSs was higher than that in the feed water (Fig. 3b). This was most pronounced in the system without cold recovery (W_{ref}). HNA cells are associated with active biomass (Lebaron et al., 2001) and primary colonizers (Proctor et al., 2018). Indeed, higher relative abundance of these groups (primary colonizers-Fig. 5) was observed in the bulk water in the pilot DSs, from day 7 to day 77. The increased presence of these groups in the bulk water is possibly linked to the fast growth of biomass and proliferation of primary colonizers (*Betaproteobacteriales*, *Pseudomonadales*, *Sphingomonadales*) (Van der Kooij et al., 2018) within biofilms on the pipe surfaces.

Furthermore, the presence of a biofilm associated bacterial group (*Sphingomonadales*), only in effluent water (W_{ref}, $W_{25°C}$, $W_{30°C}$) of the DSs and not in the feed water, shows the detachment of these cells from biofilm into the bulk water. This is confirmed by the results of the microbial source tracking (Fig. 6), where microbial communities of biofilms (Bf_{ref}, $Bf_{25°C}$, $Bf_{30°C}$) along with feed water communities showed a relevant contribution to the effluent water from all three DSs. The increased contribution from biofilms coincided with the initial maximum biomass growth within the biofilms. In the system without cold recovery (W_{ref}) these were observed later (on day 49, between day 98 and day 112 and from day 140 to day 182) than in the 25 °C and 30 °C systems (on day 21, day 49 and from day 140 to day 182 (25 °C) and from day 196 to day 220 (30 °C)). The biofilm in the reference system was relatively dense for a longer period, during which increased ATP and HNA were observed in the bulk water (W_{ref}). Thus it can be inferred that it took a longer period to form more stable biofilms in terms of detachment.

The microbial composition of the bulk water was largely determined by the composition of the feed water as revealed by the source tracking, which showed remarkable fluctuations in numbers of OTUs and in diversity. The higher numbers of OTUs within the feed water on different days of study (day 21, 49, 98, 112, 140 and 182, Fig. S5a) did not affect ATP concentrations and cell numbers for all three systems, and similar abundance and diversity were observed in effluent water of the DSs after cold recovery and the reference system. Overall, similar microbial groups were present in the feed water (Fig. S7) but with different relative abundances on different days of the study (Fig. 5). It is noted that the upstream treatment processes (biologically activated carbon filtration and slow sand filtration) contain biofilms that are allowed to mature over long periods of time. The fluctuating microbial composition of water after treatment with slow sand filtration was previously described (Bai et al., 2013; Oh et al., 2018), and is linked to scraping the schmutzdecke layer while periodically changing the sand filters, resulting in varying microbial composition, evenness and diversity of effluent water from the treatment plant (Chan et al., 2018; Haig et al., 2015).

Overall, cold recovery with subsequent increase in temperature to 25 and 30 °C showed no negative effects on microbial drinking water quality parameters (ATP, TCC) as compared to the reference. The observed changes in bulk water characteristics relative to the feed water were mostly linked with formation and growth of biofilms on pipe surface, during initial growth and decline periods (day 7–77). However,

there were some differences in water after the cold recovery systems compared to the feed water and the reference water, for example the presence of specific OTUs (*Methyloversatilis*, *Sphingobium*, *Sphingomonas*). The occurrence of *Methyloversatilis* is possibly related to its utilization of low molecular weight carboxylic acids released from pipe surfaces under warm water conditions (Smalley et al., 2015; Van der Kooij et al., 2018). However, this bacterium's nutritional conditions and growth kinetics are not studied here and require further research. Further, the *Sphingobium* and *Sphingomonas* are relevant to biofilm formation and colonization of bacteria on pipe surface (Costerton et al., 1995; Flemming et al., 2016), which caused their regrowth in the water phase within the pilot DSs.

4.3. Practical implications for water utilities

Our study showed how cold recovery, or increase in temperature, influenced the microbiology within DWDSs, such as faster primary colonization by *Betaproteobacteriales*. These may serve as prey for amoeba (Van der Kooij et al., 2018), which is followed by the simultaneous occurrence of amoeba resistant microbial groups (*Xanthobacteraceae*, *Legionellales*) in the biofilms. In contrast to observations from biofilms, *Legionellales* were not found in bulk water samples, but their persistent presence in the biofilms (within the DSs operated at 25 and 30 °C till day 232) might lead to a regrowth problem in the bulk water under favourable circumstances of higher temperature after cold recovery. Also the presence of *Pseudomonas* (in the feed water, as well as in the pilot DSs) as a core OTU among all water samples and their regrowth in biofilms needs to be closely monitored while applying cold recovery.

Hence, based on our findings new drinking water distribution systems need to be monitored more frequently within the first 2–3 months of applying cold recovery for possible effects on water quality parameters, like ATP, TCC (especially HNA cells) as well as for opportunistic pathogens like some species of *Legionella* and *Pseudomonas*. This is similar to the transition effects of changing quality of the feed water (Chen et al., 2020), where it was also suggested to monitor the system for a period of six months during which the system is restabilized in terms of microbiological water quality. The application of cold recovery in existing DWDSs which are already in operation since many years or decades may similarly require a comparable transition period to achieve stable and uniform microbiological characteristics in terms of water quality, biofilm development and habitat formation inside the pipes.

5. Conclusion

- Cold recovery from drinking water results in a subsequent increase of the drinking water temperature. The higher the water temperature after cold recovery, the faster the primary colonization stage of biofilm development.
- Higher temperatures did not lead to higher biomass density or differences in diversity in the biofilm.
- The primary colonization stage of biofilm development on new pipes led to increased biomass activity (ATP) and, specifically, increased numbers of HNA cells within the water phase, which was most pronounced in the reference system without cold recovery.
- DWDSs need to be monitored more frequently for microbiological water quality, after start of the application of cold recovery in terms of microbial composition and diversity during the first 2–3 months of operation.

Credit author statement

Jawairia Imtiaz Ahmad: Conceptualization, writing—review and editing. **Marco Dignum**: Conceptualization, writing—review and editing. **Gang Liu**: Conceptualization, writing—review and editing. **Gertjan Medema**: Conceptualization, writing—review and editing. **Jan Peter van der Hoek**: Conceptualization, writing—review and editing. All authors have read and agreed to the published version of the manuscript.

Declaration of competing interest

The authors declare that they have no known competing financial interests or personal relationships that could have appeared to influence the work reported in this paper.

Appendix A. Supplementary data

Supplementary data to this article can be found online at https://doi.org/10.1016/j.envres.2020.110648.

References

Ahmad, J.I., Liu, G., Van der Wielen, P.W.J.J., Medema, G., Van der Hoek, J.P., 2020. Effects of cold recovery technology on the microbial drinking water quality in unchlorinated distribution systems. Environ. Res. 183, 109175.

Baghoth, S.A., Sharma, S.K., Amy, G.L., 2011. Tracking natural organic matter (NOM) in a drinking water treatment plant using fluorescence excitation–emission matrices and PARAFAC. Water Res. 45 (2), 797–809.

Bai, Y., Liu, R., Liang, J., Qu, J., 2013. Integrated metagenomic and physiochemical analyses to evaluate the potential role of microbes in the sand filter of a drinking water treatment system. Public Library of Science 8 (4), e61011.

Balkwill, D.l., Fredrickson, J.K., Romine, M.F., 2006. In: Rosenberg, Eugene, Karl-Heinz Schleifer, E.S.E. (Eds.), The Prokaryotes. Martin Dworkin (Editor-In-Chief). Springer International Publishing, Singapore.

Bolyen, E., Rideout, J.R., Dillon, M.R., Bokulich, N.A., Abnet, C.C., Al-Ghalith, G.A., Alexander, H., Alm, E.J., Arumugam, M., Asnicar, F., Bai, Y., Bisanz, J.E., Bittinger, K., Brejnrod, A., Brislawn, C.J., Brown, C.T., Callahan, B.J., Caraballo-Rodríguez, A.M., Chase, J., Cope, E.K., Da Silva, R., Diener, C., Dorrestein, P.C., Douglas, G.M., Durall, D.M., Duvallet, C., Edwardson, C.F., Ernst, M., Estaki, M., Fouquier, J., Gauglitz, J.M., Gibbons, S.M., Gibson, D.L., Gonzalez, A., Gorlick, K., Guo, J., Hillmann, B., Holmes, S., Holste, H., Huttenhower, C., Huttley, G.A., Janssen, S., Jarmusch, A.K., Jiang, L., Kaehler, B.D., Kang, K.B., Keefe, C.R., Keim, P., Kelley, S.T., Knights, D., Koester, I., Kosciolek, T., Kreps, J., Langille, M.G.I., Lee, J., Ley, R., Liu, Y.-X., Loftfield, E., Lozupone, C., Maher, M., Marotz, C., Martin, B.D., McDonald, D., McIver, L.J., Melnik, A.V., Metcalf, J.L., Morgan, S.C., Morton, J.T., Naimey, A.T., Navas-Molina, J.A., Nothias, L.F., Orchanian, S.B., Pearson, T., Peoples, S.L., Petras, D., Preuss, M.L., Pruesse, E., Rasmussen, L.B., Rivers, A., Robeson, M.S., Rosenthal, P., Segata, N., Shaffer, M., Shiffer, A., Sinha, R., Song, S.J., Spear, J.R., Swafford, A.D., Thompson, L.R., Torres, P.J., Trinh, P., Tripathi, A., Turnbaugh, P.J., Ul-Hasan, S., van der Hooft, J.J.J., Vargas, F., Vázquez-Baeza, Y., Vogtmann, E., von Hippel, M., Walters, W., Wan, Y., Wang, M., Warren, J., Weber, K. C., Williamson, C.H.D., Willis, A.D., Xu, Z.Z., Zaneveld, J.R., Zhang, Y., Zhu, Q., Knight, R., Caporaso, J.G., 2019. Reproducible, interactive, scalable and extensible microbiome data science using QIIME 2. Nat. Biotechnol. 37 (8), 852–857.

Callahan, B.J., McMurdie, P.J., Rosen, M.J., Han, A.W., Johnson, A.J.A., Holmes, S.P., 2016. DADA2: high-resolution sample inference from Illumina amplicon data. Nat. Methods 13, 581.

Chan, S., Pullerits, K., Riechelmann, J., Persson, K.M., Rådström, P., Paul, C.J., 2018. Monitoring biofilm function in new and matured full-scale slow sand filters using flow cytometric histogram image comparison (CHIC). Water Res. 138, 27–36.

Chen, L., Ling, F., Bakker, G., Liu, W.-T., Medema, G., Van der Meer, W., Liu, G., 2020. Assessing the transition effects in a drinking water distribution system caused by changing supply water quality: an indirect approach by characterizing suspended solids. Water Res. 168, 115–159.

Costerton, J.W., Lewandowski, Z., Caldwell, D.E., Korber, D.R., Lappin-Scott, H.M., 1995. Microbial biofilms. Annu. Rev. Microbiol. 49 (1), 711–745.

Diaz Villanueva, V., Font, J., Schwartz, T., Romani, A.M., 2011. Biofilm formation at warming temperature: acceleration of microbial colonization and microbial interactive effects. Biofouling 27 (1), 59–71.

Douterelo, I., Sharpe, R., Boxall, J., 2013. Influence of hydraulic regimes on bacterial community structure and composition in an experimental drinking water distribution system. Water Res. 47 (2), 503–516.

El-Chakhtoura, J., Prest, E., Saikaly, P., Van Loosdrecht, M., Hammes, F., Vrouwenvelder, H., 2015. Dynamics of bacterial communities before and after distribution in a full-scale drinking water network. Water Res. 74, 180–190.

Fish, K.E., Osborn, A.M., Boxall, J., 2016. Characterising and understanding the impact of microbial biofilms and the extracellular polymeric substance (EPS) matrix in

drinking water distribution systems. Environ. Sci. Water Res. Technol. 2 (4), 614–630.

Flemming, H.-C., Wingender, J., Szewzyk, U., Steinberg, P., Rice, S.A., Kjelleberg, S., 2016. Biofilms: an emergent form of bacterial life. Nat. Rev. Microbiol. 14, 563.

Haig, S.-J., Quince, C., Davies, R.L., Dorea, C.C., Collins, G., 2015. The relationship between microbial community evenness and function in slow sand filters. mBio 6 (5).

Henne, K., Kahlisch, L., Brettar, I., Hofle, M.G., 2012. Analysis of structure and composition of bacterial core communities in mature drinking water biofilms and bulk water of a citywide network in Germany. Appl. Environ. Microbiol. 78 (10), 3530–3538.

Hull, N.M., Ling, F., Pinto, A.J., Albertsen, M., Jang, H.G., Hong, P.-Y., Konstantinidis, K. T., LeChevallier, M., Colwell, R.R., Liu, W.-T., 2019. Drinking water microbiome project: is it time? Trends Microbiol. 27 (8), 670–677.

Kelly, J.J., Minalt, N., Culotti, A., Pryor, M., Packman, A., 2014. Temporal variations in the abundance and composition of biofilm communities colonizing drinking water distribution pipes. Public Library of Science 9 (5), e98542.

Knights, D., Kuczynski, J., Charlson, E.S., Zaneveld, J., Mozer, M.C., Collman, R.G., Bushman, F.D., Knight, R., Kelley, S.T., 2011. Bayesian community-wide culture-independent microbial source tracking. Nat. Methods 8 (9), 761–763.

Lebaron, P., Servais, P., Agogué, H., Courties, C., Joux, F., 2001. Does the high nucleic acid content of individual bacterial cells allow us to discriminate between active cells and inactive cells in aquatic systems? Appl. Environ. Microbiol. 67 (4), 1775–1782.

Ling, F., Hwang, C., LeChevallier, M.W., Andersen, G.L., Liu, W.-T., 2015. Core-satellite populations and seasonality of water meter biofilms in a metropolitan drinking water distribution system. ISME J. 10, 582.

Ling, F., Whitaker, R., LeChevallier, M.W., Liu, W.-T., 2018. Drinking water microbiome assembly induced by water stagnation. ISME J. 12 (6), 1520–1531.

Liu, G., Bakker, G.L., Li, S., Vreeburg, J.H.G., Verberk, J.Q.J.C., Medema, G.J., Liu, W.T., Van Dijk, J.C., 2014. Pyrosequencing reveals bacterial communities in unchlorinated drinking water distribution system: an integral study of bulk water, suspended solids, loose deposits, and pipe wall biofilm. Environ. Sci. Technol. 48 (10), 5467–5476.

Liu, G., Tao, Y., Zhang, Y., Lut, M., Knibbe, W.-J., van der Wielen, P., Liu, W., Medema, G., van der Meer, W., 2017. Hotspots for selected metal elements and microbes accumulation and the corresponding water quality deterioration potential in an unchlorinated drinking water distribution system. Water Res. 124, 435–445.

Liu, G., Verberk, J.Q.J.C., Van Dijk, J.C., 2013. Bacteriology of drinking water distribution systems: an integral and multidimensional review. Appl. Microbiol. Biotechnol. 97 (21), 9265–9276.

Liu, G., Zhang, Y., Van der Mark, E., Magic-Knezev, A., Pinto, A., Van den Bogert, B., Liu, W., Van der Meer, W., Medema, G., 2018. Assessing the origin of bacteria in tap water and distribution system in an unchlorinated drinking water system by SourceTracker using microbial community fingerprints. Water Res. 138, 86–96.

Magic-Knezev, A., van der Kooij, D., 2004. Optimisation and significance of ATP analysis for measuring active biomass in granular activated carbon filters used in water treatment. Water Res. 38 (18), 3971–3979.

Mathieu, L., Paris, T., Block, J.-C., 2019. In: Hurst, C.J. (Ed.), The Structure and Function of Aquatic Microbial Communities. Springer International Publishing, Cham, pp. 261–311.

Mol, S., Kornman, J., Kerpershoek, A., Van Der Helm, A., 2011. Opportunities for public water utilities in the market of energy from water. Water Sci. Technol. 63 (12).

Neu, L., Proctor, C.R., Walser, J.-C., Hammes, F., 2019. Small-scale heterogeneity in drinking water biofilms. Front. Microbiol. 10 (2446).

Oh, S., Hammes, F., Liu, W.-T., 2018. Metagenomic characterization of biofilter microbial communities in a full-scale drinking water treatment plant. Water Res. 128, 278–285.

Potgieter, S., Pinto, A., Sigudu, M., Du Preez, H., Ncube, E., Venter, S., 2018. Long-term spatial and temporal microbial community dynamics in a large-scale drinking water distribution system with multiple disinfectant regimes. Water Res. 139, 406–419.

Prest, E.I., Hammes, F., Kötzsch, S., Van Loosdrecht, M.C.M., Vrouwenvelder, J.S., 2013. Monitoring microbiological changes in drinking water systems using a fast and reproducible flow cytometric method. Water Res. 47 (19), 7131–7142.

Prest, E.I., Hammes, F., Van Loosdrecht, M.C.M., Vrouwenvelder, J.S., 2016a. Biological stability of drinking water: controlling factors, methods, and challenges. Front. Microbiol. 7, 45.

Prest, E.I., Weissbrodt, D.G., Hammes, F., Van Loosdrecht, M.C.M., Vrouwenvelder, J.S., 2016b. Long-term bacterial dynamics in a full-scale drinking water distribution system. Public Library of Science 11 (10), e0164445.

Proctor, C.R., Besmer, M.D., Langenegger, T., Beck, K., Walser, J.-C., Ackermann, M., Bürgmann, H., Hammes, F., 2018. Phylogenetic clustering of small low nucleic-content bacteria across diverse freshwater ecosystems. ISME J. 12 (5), 1344–1359.

Rogers, J., Dowsett, A.B., Dennis, P.J., Lee, J.V., Keevil, C.W., 1994. Influence of temperature and plumbing material selection on biofilm formation and growth of Legionella pneumophila in a model potable water system containing complex microbial flora. Appl. Environ. Microbiol. 60.

Smalley, N.E., Taipale, S., De Marco, P., Doronina, N.V., Kyrpides, N., Shapiro, N., Woyke, T., Kalyuzhnaya, M.G., 2015. Functional and genomic diversity of methylotrophic Rhodocyclaceae: description of Methyloversatilis discipulorum sp. nov. Int. J. Syst. Evol. Microbiol. 65 (7), 2227–2233.

Smeets, P., Medema, G., Van Dijk, J., 2009. The Dutch secret: how to provide safe drinking water without chlorine in The Netherlands. Drink. Water Eng. Sci. 2 (1), 1–14.

Staatscourant, 2011. Staatscourant (State Journal in Dutch) 2011 Decree of 23 May 2011 Concerning the Regulations for the Production and Distribution of Drinking Water and the Organisation of the Public Drinking Water Supply (The Netherlands).

Thijs, S., Op De Beeck, M., Beckers, B., Truyens, S., Stevens, V., Van Hamme, J.D., Weyens, N., Vangronsveld, J., 2017. Comparative evaluation of four bacteria-specific primer pairs for 16S rRNA gene surveys. Front. Microbiol. 8, 494.

Van der Hoek, J.P., Mol, S., Giorgi, S., Ahmad, J.I., Liu, G., Medema, G., 2018. Energy recovery from the water cycle: thermal energy from drinking water. Energy 162, 977–987.

Van der Kooij, D., 1992. Assimilable organic carbon as an indicator of bacterial regrowth. J. Am. Water Works Assoc. 84 (2), 57–65.

Van der Kooij, D., Van der Wielen, P.W., 2013. Microbial growth in drinking-water supplies: problems, causes, control and research needs. Water Intell. Online 12.

Van der Kooij, D., Veenendaal, H.R., Italiaander, R., Van der Mark, E.J., Dignum, M., 2018. Primary colonizing Betaproteobacteriales play a key role in the growth of Legionella pneumophila in biofilms on surfaces exposed to drinking water treated by slow sand filtration. Appl. Environ. Microbiol. 84 (24).

Van Der Wende, E., Characklis, W.G., Smith, D.B., 1989. Biofilms and bacterial drinking water quality. Water Res. 23 (10), 1313–1322.

Vital, M., Dignum, M., Magic-Knezev, A., Ross, P., Rietveld, L., Hammes, F., 2012. Flow cytometry and adenosine tri-phosphate analysis: alternative possibilities to evaluate major bacteriological changes in drinking water treatment and distribution systems. Water Res. 46 (15), 4665–4676.

Wingender, J., Flemming, H.-C., 2011. Biofilms in drinking water and their role as reservoir for pathogens. Int. J. Hyg Environ. Health 214 (6), 417–423.

Zhou, X., Ahmad, J.I., van der Hoek, J.P., Zhang, K., 2020. Thermal energy recovery from chlorinated drinking water distribution systems: effect on chlorine and microbial water and biofilm characteristics. Environ. Res. 187, 109655.

Zhou, X., Zhang, K., Zhang, T., Li, C., Mao, X., 2017. An ignored and potential source of taste and odor (T&O) issues-biofilms in drinking water distribution system (DWDS). Appl. Microbiol. Biotechnol. 101 (9), 3537–3550.

Zlatanović, L., Van der Hoek, J.P., Vreeburg, J.H.G., 2017. An experimental study on the influence of water stagnation and temperature change on water quality in a full-scale domestic drinking water system. Water Res. 123, 761–772.